Stereoselective non-equivalent bis-diimine coordination to Co(II) ion: Structure, luminescence and density functional theory calculations

Amit Saha Roy [a], Manas Kumar Biswas [a], Thomas Weyhermüller [b], Prasanta Ghosh [a,*]

[a] Department of Chemistry, R.K. Mission Residential College, Narendrapur, Kolkata 103, India
[b] Max-Planck-Institut für Bioanorganische Chemie, Stiftstrasse 34-36, D-45470, Mülheim an der Ruhr, Germany

ARTICLE INFO

ABSTRACT

Stereoselective coordination affording a luminescent *tcc*-isomer of dihalobis(diimine)Co(II) family in which two photoactive diimine ligands (L_{NO2}^{ϕ}) are unsymmetrical and non-equivalent is reported (L_{NO2}^{ϕ} = (*E*)-3-nitro-*N*-(pyridine-2-ylmethylene)aniline; ϕ = dihedral angle between the diimine unit including pyridine ring and the phenyl ring planes; *tcc* refers *trans–cis–cis* positions with respect to pyridine nitrogen-imine nitrogen-chloride donors). The single step reaction of 2-pyridinecarboxaldehyde, 3-nitro aniline and anhydrous cobalt dichloride affords only the *tcc*-$(L_{NO2}^{\phi 1})(L_{NO2}^{\phi 2})Co^{II}Cl_2$ as the product which is characterized by IR, Mass, UV–Vis spectra and magnetic susceptibility measurements. Single crystal X-ray structure determination has established the orientation of the two ligands in the crystal as $(L_{NO2}^{33.7})(L_{NO2}^{79.7})Co^{II}Cl_2 \cdot 0.25CH_3OH$ (**1**). The isomer is luminescent in frozen methanol glass at 77 K with the excitation and emission maxima respectively at 370 and 525 nm. The average luminescence life time is 1.86 ns measured on exciting at 356 nm. Density functional theory (DFT) calculation shows that the non-equivalence of the two diimine ligands prevails in the gas phase also and the geometry is $(L_{NO2}^{41.0})(L_{NO2}^{60.5})Co^{II}Cl_2$. The calculation has identified four types of closely spaced localized π^* orbitals as unoccupied photoactive molecular orbitals (UPMOs). TD-DFT calculations have assigned the Co(II) to π^* charge transfer (MLCT) and π to π^* of charge transfer (LLCT) as the primary origin of absorption above 340 nm in methanol. Pendant nitro groups of the ligands and their intermolecular interactions have been the driving force of the stereoselectivity of the product. The binuclear $L_4Co_2Cl_4$ unit of **1** has constructed the helical 2D assembly and *cis*-CoCl$_2$ mediated strong inter-helices H-bonding interactions result the channeled 3D framework. Geometry optimization of other possible *ttt, ctc, ccc* and *cct* isomers has established that in the gas phase, the *tcc*-isomer is more stable at least by 20–42 kJ mol^{-1} compared to other isomers where the two diimine ligands are equivalent.

© 2010 Elsevier B.V. All rights reserved.

1. Introduction

Metal bound α-diimine chromophore is photoactive [1–9]. Possibility of easy electron transfer to the low-lying π^* orbital, an important unoccupied photoactive molecular orbital (UPMO), of the coordinated α-diimine skeleton, in many cases even generating diimine anion radical [10–13], makes transition metal diimine species a special group of MLCT series. An assortment of the photo-physical properties of such molecule is possible by tuning the conjugation of the photoactive π^* orbital of the α-diimine core and substitution. Two most strong and rigid chelating heterocyclic α-diimines are 2,2′-bipyridine (bpy) and 1,10-phenanthroline (phen) which form tris(diimine), ML_3^{3+} type or bis(diimine), L_2MX_2 type of species (L = bpy, phen; X = halogens) with transition metal ions. In each case, the two or three coordinated heterocyclic diimines around the metal center remain equivalent keeping the components of the photoactive $\pi_{diimine}$ or $\pi_{diimine}^*$ orbitals unperturbed. For a bis or poly diimine coordinated system, to have the discrete energy levels due to π or π^* orbitals, tuning of the constituents of these photoactive orbitals of each diimine unit is required. Two or more non-equivalent diimines around a metal center potentially can have closely spaced localized π^* orbitals as LUMOs that accept charge counting higher dipole moment change and prompts new photoactivities.

To achieve such molecular composition, one of the prerequisites is the coordination of an unsymmetrical diimine fragment. To our knowledge, not a single coordination compound of dichlorobis(diimine)M(II) series with 3d-metal ion incorporating two non-equivalent unsymmetrical diimine ligands has been reported so far. In this article, we report the synthesis, structure, spectra and the density functional theory calculations of a luminescent *tcc*-isomer of this family in which two diimine ligands are unsymmetrical and non-equivalent. The isomer is shown in Chart

---

* Corresponding author. Tel.: +91 33 2428 7017; fax: +91 33 2477 3597.
  E-mail address: ghoshp_chem@yahoo.co.in (P. Ghosh).

1 and abbreviated as *tcc*-(L$_{NO2}^{\phi 1}$)(L$_{NO2}^{\phi 2}$)Co^{II}Cl$_2$ (L$_{NO2}^{\phi}$ = (*E*)-3-nitro-*N*-(pyridine-2-ylmethylene)aniline; φ = dihedral angle between the diimine unit including pyridine ring and the phenyl ring planes in crystals; *tcc* denotes *trans–cis–cis* positions with respect to pyridine nitrogen-imine nitrogen-chloride of the coordination sphere).

2. Experimental

2.1. Material and physical measurements

Reagents or analytical grade materials were obtained from commercial suppliers and used without further purification. Spectroscopic grade solvents were used for spectroscopic and electrochemical measurements. The C, H and N content of the compounds were obtained from *Perkin–Elmer 2400 series II* elemental analyzer. Infrared spectra of the samples were measured from 4000 to 400 cm^{-1} with the KBr pellet at room temperature on a *Perkin–Elmer FT-IR-Spectrophotometer Spectrum RX 1*. Electronic absorption spectrum in solution at 298 K was carried out on a *Perkin–Elmer Lambda 25* spectrophotometer in the range of 1100–200 nm. The temperature-dependent magnetic susceptibility of the solid sample of **1** has been measured by using SQUID magnetometer. Emission spectrum at 77 K were recorded in MeOH by using quartz sample tube on *Perkin–Elmer LS 55* fluorescence spectrophotometer equipped with a *Perkin–Elmer* low-temperature luminescence accessory.

2.2. Synthesis of tcc-(L$_{NO2}^{33.7}$)(L$_{NO2}^{79.7}$)Co^{II}Cl$_2$·0.25MeOH (**1**)

To 3-nitroaniline (280 mg, 2 mmol), pyridine-2-carboxyaldehyde (220 mg, 2 mmol) was mixed well to form a paste. To this paste methanol (25 ml) was added and heated at 50 °C and stirred for 15 min. The reaction mixture was cooled at 20 °C. To this solution mixture, anhydrous CoCl$_2$ (200 mg, 1 mmol) was added and stirred for 20 min. The solution were filtered. The dark red filtrate was collected and allowed to evaporate slowly in air. Within two days red crystals of **1** separated out, which were filtered and dried in air (single-crystals for X-ray structure were picked out from this product). Yield: 360 mg (60% with respect to cobalt). Mass spectrum (ESI, positive ion, CH$_2$Cl$_2$; *m/z*): 548.00 {**1**-(0.25CH$_3$OH + Cl)}$^+$. *Anal.* Calc. for C$_{24.25}$H$_{19}$Cl$_2$CoN$_6$O$_{4.25}$: C, 49.18; H, 3.23; N, 14.18. Found: C, 49.01; H, 3.30; N, 14.14%. IR (KBr): *v*, 1631(vs), 1594(vs), 1529(vs), 1352 (vs), 1203(m), 820(m), 782(m), 740(m), 680(m) cm^{-1}.

2.3. X-ray crystallographic data collection and refinement of the structure

Dark red single crystal of **1** was picked up with a nylon loop and was mounted in the nitrogen cold stream of a diffractometer. A
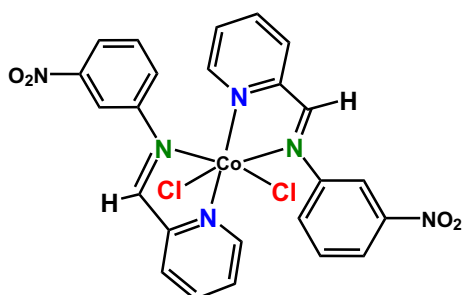
Nonius Kappa-CCD diffractometer equipped with a Mo-target rotating-anode X-ray source and a graphite monochromator (Mo Kα, λ = 0.71073 Å) was used. Final cell constants were obtained from least squares fits of all measured reflections. Intensity data were corrected for absorption using intensities of redundant reflections. The structure was readily solved by direct method and subsequent difference Fourier techniques. The crystallographic data of **1** has been listed in Table 1. The Siemens SHELXTL [14] software package was used for solution and artwork of the structure, SHELXL97 [15] was used for the refinement. All non-hydrogen atoms were refined anisotropically. Hydrogen atoms were placed at the calculated positions and refined as riding atoms with isotropic displacement parameters. The carbon and oxygen atoms of the CH$_3$OH solvent are disordered with respect to their positions and have been refined with 50% occupancies in both positions of each atom.

2.4. Density functional theory (DFT) calculations

All calculations reported in this article were done with the GAUSSIAN 03 W [16] program package supported by GaussView 4.1. The DFT [17] and TD-DFT [18] calculations have been performed at the level of Becke three parameter hybrid functional with the non-local correlation functional of Lee–Yang–Parr (B3LYP) [19]. The geometry of **1** in the gas phase has been optimized using Pualy's Direct Inversion [20] in the Iterative Subspace (DIIS), 'tight' convergent SCF procedure [21] ignoring symmetry using *S* = 3/2 spin state. In all calculation, a LANL2DZ basis set along with the corresponding effective core potential (ECP) was used for cobalt metal atom [22–24]. Basis set 6-31G [25] for H has been used. For non-hydrogen atoms first polarization functions have been added. Basis set 6-31G (d, p) [26] for C, N, O and 6-311G (d,p) [27] for Cl atoms were employed for the calculation. The geometries of *ccc, ttt, cct* and *ctc* isomers have also been optimized using DIIS and 'tight' convergence in SCF for comparison. The geometry of *cct* isomer failed to converge because of crowding and unexpected bonding interactions. The percentage contribution of metal, chloride and ligands of the frontier orbitals of **1**, have been calculated using GAUSSSUM program package [28]. The eighty lowest singlet excitation energies on the optimized geometry of **1** in methanol have been calculated by TD-DFT method using conductor-like polarizable continuum model (CPCM) [29]. The nature of

Chart 1. *tcc*-(L$_{NO2}^{\phi 1}$)(L$_{NO2}^{\phi 2}$)Co^{II}Cl$_2$.

Table 1
Crystallographic data for **1**.

Chemical Formula	C$_{24.25}$H$_{19}$Cl$_2$CoN$_6$O$_{4.25}$
F$_w$	592.28
Space group	*P*2$_1$/c
a (Å)	12.5283(4)
b (Å)	13.9515(4)
c (Å)	15.1723(4)
β, deg	112.885(3)
V (Å)	2443.2 (12)
Z	4
T (K)	100(2)
D$_{calc}$ (g cm^{-3})	1.610
Reflections collected/2θ$_{max}$	56068/65
Unique reflections	8829
Number of parameters/restraints	343/0
λ (Å)/μ, (mm^{-1})	0.71073/0.968
R_1 [a]/goodness of fit (GOF) [b]	0.0295/1.028
wR_2 [c] ($I > 2\sigma(I)$)	0.0749
Residual density (e Å^{-3})	1.117

Observation criterion: $I > 2\sigma(I)$.
[a] $R_1 = \sum ||F_o| - |F_c||/\sum |F_o|$.
[b] GOF = $\{\sum[w(F_o^2 - F_c^2)^2]/(n - p)\}^{1/2}$.
[c] $wR_2 = [\sum[w(F_o^2 - F_c^2)^2]/\sum[w(F_o^2)^2]]^{1/2}$, where $w = 1/[\sigma^2(F_o^2)+(aP)^2 + bP]$, $P = (F_o^2 + 2F_c^2)/3$.

transition has been calculated by adding the probability of same type among alpha and beta molecular orbitals.

3. Results and discussion

3.1. Synthesis of complex

Out of possible five isomers with respect to *tans* and *cis* positions of the pyridine nitrogen, imine nitrogen and chloride donors, the only compound isolated is *tcc*-$(L_{NO2}^{33.7})(L_{NO2}^{79.7})Co^{II}Cl_2 \cdot$ 0.25MeOH (**1**), geometry of which is shown in Chart 1. The L_{NO2}^{ϕ} ligand has not been pre-isolated. The crystalline compound **1** was prepared in high yield in a single step reaction using the mixture of 2-pyridinecarboxaldehyde, 3-nitroaniline and anhydrous metal dichloride in methanol as solvent at room temperature. The unsubstituted aniline in similar condition does not afford any product. We failed to isolate any product even with 2-nitro or 4-nitroanilines. It is noteworthy that the reaction is stereoselective and only the pure *tcc*-isomer of possible five stereoisomers crystallizes from the reaction mixture. The quartet spin state of **1** has been confirmed by the variable temperature magnetic susceptibility measurement as shown in Fig. 1.

3.1.1. Molecular structure

The *tcc* geometry of **1** has been confirmed by the single crystal X-ray structure determination at 100 K. An ortep plot of the isomer has been shown in Fig. 2. Selected bond parameters are listed in Table 2. In **1**, the average Co–N (pyridine) distance, 2.1521(10) Å is shorter than the average Co–N(imine) distance, 2.2136(10) Å. The Cl–Co–Cl, angle is 99.363(12)°.

The X-ray structure shows the non-equivalence of the two diimine ligands. The values of the dihedral angle (ϕ) are 33.7 and 79.7 and the two ligands are abbreviated as $L_{NO2}^{33.7}$ and $L_{NO2}^{79.7}$ as in Fig. 2. In **1**, the diimine unit including the pyridine ring (A) of $L_{NO2}^{33.7}$ forms a good plane of mean deviation around 0.01 Å. In $L_{NO2}^{79.7}$, the mean deviation of the plane of the diimine fragment with the pyridine ring (C) is about 0.05 Å. Calculation on free ligand (L_{NO2}^{ϕ}) has established that at the orientation of $\phi = 90°$, the π^* orbital as LUMO of the ligand will be destabilized the most. In **1**, the π^* orbital of the $L_{NO2}^{79.7}$ will be more destabilized compared to $L_{NO2}^{33.7}$ leading to two distinct UPMOs. Such molecular orientation has been forced to avoid the interaction between the two aromatic rings. To minimize the crowding, pyridine (A) and the 3-nitrophenyl (D) rings remain parallel. The distance between the centers of these two rings is 4.259 Å.
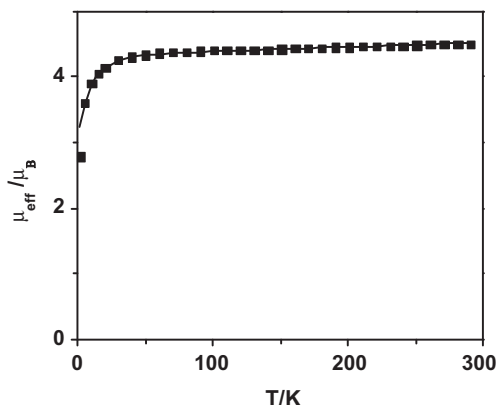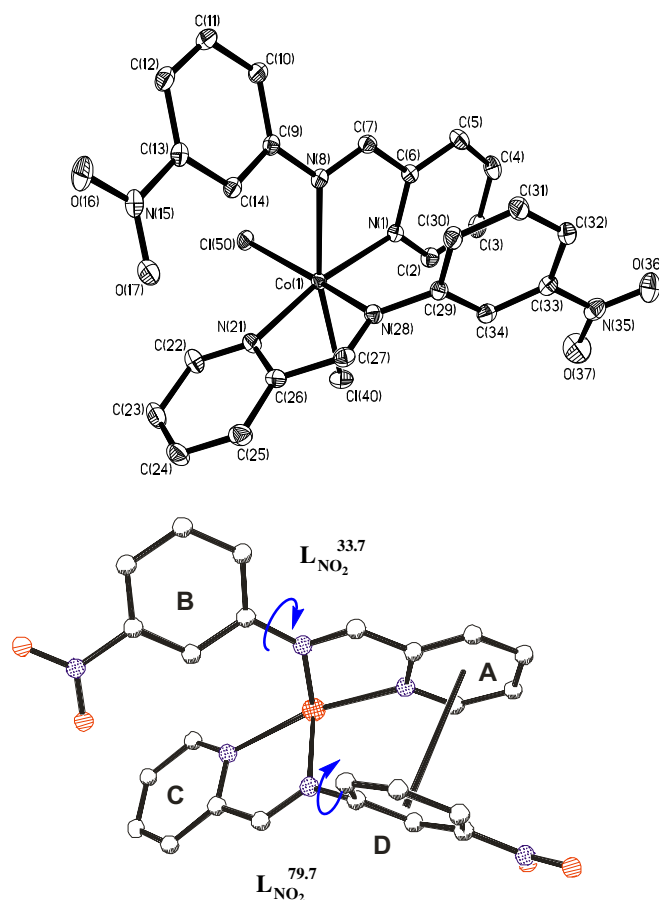

Fig. 2. ORTEP plot of **1** (50% thermal ellipsoids and solvent MeOH has been omitted) (top) and non-equivalent orientation of the phenyl rings with respect to the diimine chelate in two ligands (bottom).

Table 2
Selected bond lengths (Å) and angles (°) of **1**.

Co1–N1	2.146(10)	Co1–Cl50	2.3529(3)
Co1–N21	2.158(10)	N1–Co1–N21	167.52(4)
Co1–N8	2.2514(10)	N28–Co1–Cl50	163.48(3)
Co1–N28	2.1759(10)	N8–Co1–Cl40	167.18(3)
Co1–Cl40	2.4156(3)	Cl50–Co1–Cl40	99.36(12)

3.1.2. Stereoselectivity and non-bonding assemblies

Two unsymmetrical diimines and two halides ions around a metal center can have total five isomers but the reaction mixture here affords only the *tcc*-isomer as the product. Analysis of crystal packing shows strong intermolecular non-bonding interactions that furnishes 2D and 3D assembly of this isomer. The non-bonding assemblies have been realized because of the (i) pendent NO_2–NO_2, (ii) NO_2–H (aromatic), (iii) *cis*-CoCl$_2$–MeOH(solvent), (iv) *cis*-MCl$_2$ H(aldimine), (v) *cis*-CoCl$_2$–H(aromatic) and (vi) MeOH–H non-bonding interactions. The different types of effective intermolecular non-bonding lengths of **1** have been listed in Table 3. A

Fig. 1. Variable temperature magnetic moment, $\mu_{eff, }\mu_B$, of **1**.

Table 3
Significant weak bonding distances (Å) in **1**.

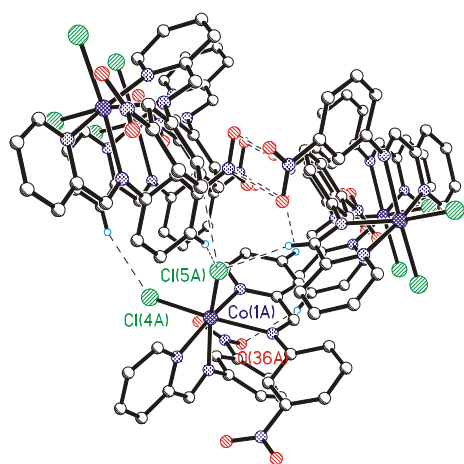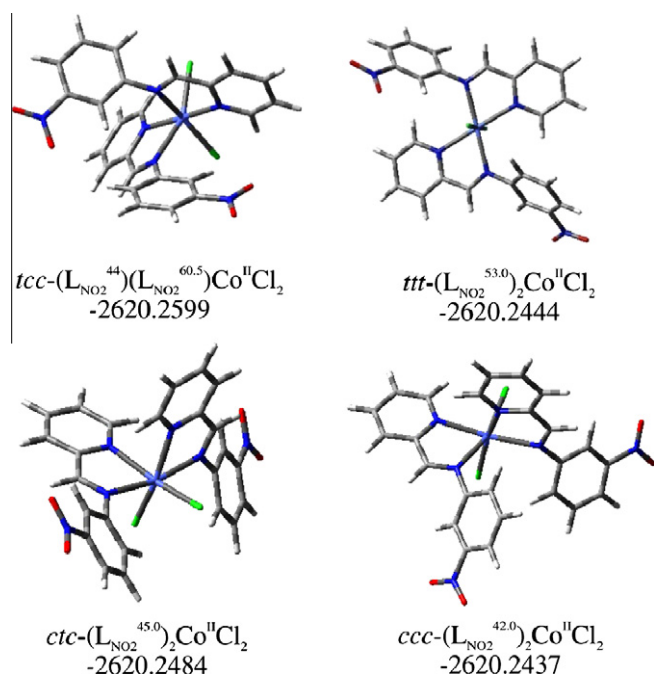|			
O17–N15	2.910	H5–Cl40	2.792
H7–O(MeOH)	2.278	H12–Cl50	2.661
H4–O17	2.445	H23–Cl40	2.803
H24–O36	2.542	H27–Cl50	2.618
H10–O(MeOH)	2.383	O(MeOH)–Cl40	3.007
H34–O(MeOH)	2.392		

Fig. 3. Centrosymmetric $L_4Co_2Cl_4$ unit and inter-helices H-bondings.

Scheme 1. Optimized geometries and energies (a.u.) of all possible isomers in the gas phase.

dinuclear assembly has been the building block of the 3D construction in crystal of **1**. Here, the dipole–diploe interactions among the –NO$_2$ groups generate the centrosymmetric dinuclear $L_4Co_2Cl_4$ unit as in Fig. 3. Strong H-bonding of the *cis*-dichlorocobalt(II) unit with the aromatic H-atoms and MeOH solvent stabilize the 2D array. The 2D assemblies are helical in nature and assemble to a channeled 3D architecture by strong inter-helices H-bonding interactions. In this context, *cis*-CoCl$_2$ unit plays an important role and acts like a 'Molecular Stand' holding two dinuclear units, of other helix by H-bonding interactions.

3.1.3. The gas phase geometry

In soild state, the formation of only *tcc*-isomer has been confirmed by single crystal X-ray structure determinations of **1**. To know the trend in the gas phase, geometries of other possible *ctc*, *ccc*, *ttt* and *cct* isomers have been optimized by density functional theory (DFT) calculations at the unrestricted B3LYP level using $S = 3/2$ spin state. The calculations show that compared to *ctc*, *ttt*, and *ccc* isomers, *tcc*-isomer is stabilized at least by 30, 40 and 42 kJ/mol, respectively, as in Scheme 1. The minimum energy of the *tcc* isomer correlates well with the experimental finding of the stereoselectivity of the isolated product. It predicts the presence of only *tcc*-isomer in solution also. Moreover, it is to be noted that in all other isomers the orientation of the pendant phenyl ring in the two diimine unit is equivalent as given in Scheme 1. Unfortunately, *cct* isomer fails to converge in SCF due to strong non-bonding interaction between two phenyl rings and it appears the least stable.

3.2. UV–Vis absorption and fluorescence spectra

The absorption feature of **1** is solvent dependent. In methanol, it displays very strong absorption bands at 300–200 nm and moderately strong band at above 300 nm. Data have been summarized in Table 4 and spectra are shown in Fig. 4. In dichloromethane solvent, the low energy band with the maxima near 370 nm is absent.

Emission spectrum of **1** in frozen methanol glass with the solution concentration in the order of 10^{-5} mol/L has been recorded at 77 K with the excitation maximum at 370 nm (Table 3). Fig. 5 displays the spectrum. The luminescence lifetime in the frozen glass of the species has been measured on exciting at 356 nm. Two component lifetimes fitted well with an average of 1.86 ns. It is to be noted that the compound is not emissive in dichloromethane solution. The origin of the absorption and luminescence has been elucidated by TD-DFT calculation and has been included in the next section.

3.3. Localization of LUMOs, excited states and excitation energies

To know the effect of the non-equivalence of the two diimine ligands in UPMOs and OPMOs, the molecule **1** in the gas phase was optimized with the quartet spin ($S = 3/2$) state without any symmetry constraint using tight convergence in SCF. The bond parameters of the optimized structure are as follows: Co–N(Py) = 2.216, 2.202; Co–N(imine) = 2.289, 2.314; Co–Cl = 2.435, 2.402; –CH=N– = 1.282, 1.280; =CH–C(Py) = 1.415, 1.414 Å. The significant difference between the calculated and experimental bond parameters of the coordination sphere may be due to the strong non-bonding interactions among the –NO$_2$ groups of the ligand in solid. The spin density distribution of optimized molecule of **1** is as follows: Co, 2.68; Cl, 0.096; N, 0.05 which are consistent with the Co(II) high spin state. In the optimized geometry of **1**, the orientations of the two phenyl rings are different as in solid state. The dihedral angle between the diimine fragment and the phenyl ring planes is 44° in one ligand, while the angle is 61° in other ligand. It correlates well with the ligands $L_{NO2}^{33.7}$ and $L_{NO2}^{79.7}$ in solid state. Therefore, in the gas phase, **1** is defined as $(L_{NO2}^{44})(L_{NO2}^{60.5})Co^{II}Cl_2$ as shown in Scheme 1. A molecular scheme with the iso-surface plot (0.04) of the significant molecular orbitals of

Table 4
Absorption spectral data of **1** in methanol, dichloromethane and emission spectral data in frozen methanol glass at 77 K.

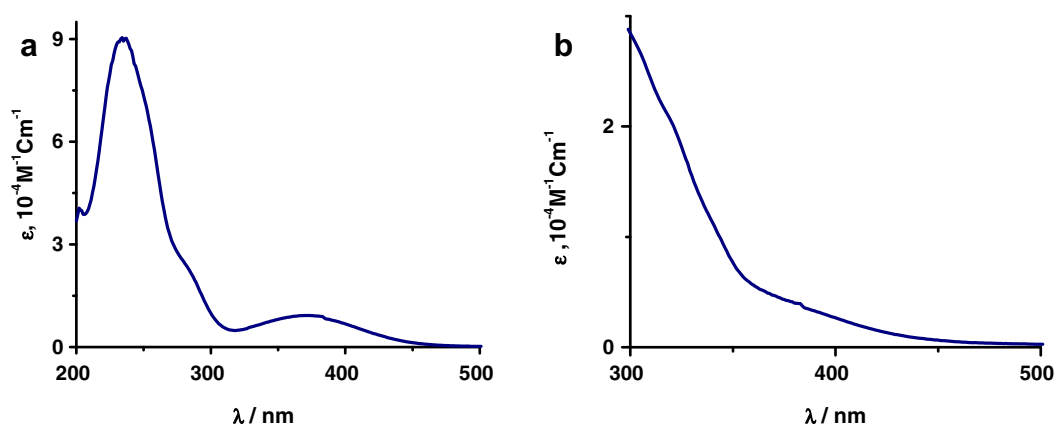| λ_{max} (nm) (ε, M^{-1}cm^{-1}) (298 K)		λ_{ext} (nm) (77 K)	λ_{em} (nm) (77 K)	Lifetime(ns) (Ext at 356 nm)	χ^2	τ_{av}
MeOH	CH$_2$Cl$_2$					
373(9168), 278(25896), 235(89540)	321 (19792)	370	529	τ_1 = 12.84(3.0%), τ_2 = 1.53(97.0%)	0.99	1.86

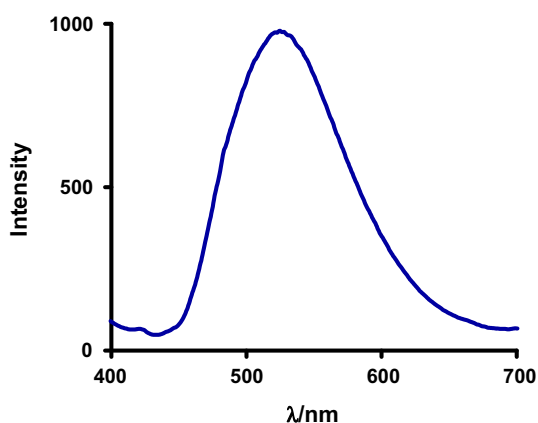**Fig. 4.** Electronic spectra of **1** (a) in MeOH (b) in dichloromethane.

Fig. 5. Emission spectrum of **1** in frozen MeOH glass at 77 K.

$(L_{NO2}{}^{44})(L_{NO2}{}^{60.5})Co^{II}Cl_2$ is displayed in Fig. 6. The constituents of the frontier orbitals are calculated using the Gaussian output files and the GAUSSSUM program package [28].

The calculations have summed up the effect of non-equivalence and the nitro substitutions of the two diimine ligands on the excited state electronic state of these complexes. The first four unoccupied molecular orbitals based on ligands are closely spaced and both the alpha and the beta LUMO being localized on the more conjugated ligand on $L_{NO2}{}^{44}$. The π^* orbital of the nitro group of the $L_{NO2}{}^{60.5}$ ligand constitutes the alpha and beta LUMO+1. The LUMO+2 (α and β) scatter mainly on the diimine fragment of $L_{NO2}{}^{60.5}$ while LUMO+3 are more localized on the nitro groups of the more conjugated $L_{NO2}{}^{44}$ ligand. The secondary effect of the nitro group is that the second excited state due to transitions from Co(II) to the nitro group of less conjugated phenyl ring of $L_{NO2}{}^{60.5}$ ligand is more like a charge separated state as $[(diimine)_2Co^{III}Cl_2]^+[NO_2Ph]^-$. The nitro group on the $L_{NO2}{}^{60.5}$ ligand having minimum conjugation with the
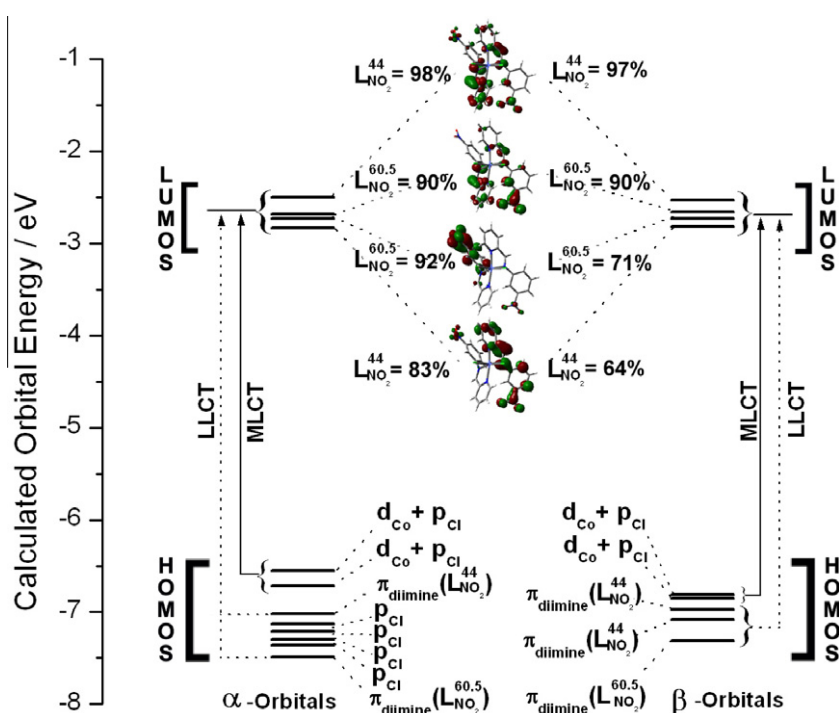

Fig. 6. A molecular orbital scheme of **1.**

Table 5
Calculated lower energy absorption maxima, λ_{cal} (nm), metal to ligand charge transfer (MLCT), ligand to ligand charge transfer (LLCT) probabilities (%) and oscillator strength (f) of **1**.

λ_{cal} (nm)	f	MLCT (%)	LLCT (%)
412	0.012	65.0	9.5
349	0.013	42.8	41.3
347	0.013	28.6	56.3
342	0.017	11.0	51.0

diimine fragment is a good acceptor here. It leads to photo induced charge-separation that is an important topic of current research [2].

The origin of the absorptions of the complex **1** in methanol has been elucidated by the theoretical calculations at the TD-DFT level using CPCM model. Analyses have found out two types of significant transitions that are summarized in Fig. 6. These are mainly metal to ligand charge transfer (MLCT) and ligand to ligand charge transfer (LLCT). Excitation energies of the transitions with oscillator strength higher than 0.010, have been listed in Table 5. As the excitation wavelength for the emission spans the range 340–380 nm, the absorption maxima more than 340 nm is worthy to investigate. The origin of calculated bands at 350, 347 and 343 nm has given an insight of the origin of these lower energy bands. Analyses of the expansion coefficients assign π to π^* and Co(II) to π^* transitions as major contributions of such absorptions as given in Table 5. Table shows that with the increase of absorption energy, the contribution of MLCT decreases. The calculated lower energy band maxima at 412 nm is mainly due to the transition from Co(II) to π^* ligand. Calculation shows that the energies of the localized π (occupied) and π^*(unoccupied) orbitals is a function of solvation. It affects the extent of stabilization or destabilization of such orbitals. In methanol, difference of energies of the π and π^* orbitals is less than that in dichloromethane. Thus, low energy transitions are absent in dichloromethane solvent and the compound has accordingly been found to be non-emissive. The free ligand is also non-emissive.[1] As it has already been established that the UPMOs are localized, energies of such orbitals are expected to be solvent dependent that is observed in the experimental spectra.

4. Summary

In summary, stereoselective coordination generating a new member of the dihalobis(diimine)M(II) family in which the two diimine ligands ($L_{NO2}{}^{\phi}$) are unsymmetrical and non-equivalent both in solid and the gas phase as in tcc-$(L_{NO2}{}^{\phi 1})(L_{NO2}{}^{\phi 2})Co^{II}Cl_2$ is reported. The facile formation of only one isomer opens up a new route to achieve unknown non-equivalent bis(diimine) species with other transition elements. Because of the non-equivalence of two diimine ligands and nitro substitution, this isomer produces a band of four closely spaced UPMOs that are localized. The complex is high spin but luminescent at 77 K in frozen methanol glass with the average luminescence lifetime 1.86 ns due to transitions to these π^* band. Optimization of geometries in the gas phase shows that in all isomers except the tcc isomer, two diimine ligands are equivalent. Tuning of substituents on the photoactive diimine chromophore to control the stereochemistry and emission property of the product appeared to be a significant area for further investigation.

---

[1] The ligand (L_{4-OH}) with 4-hydroxyaniline has been successfully isolated and characterized with IR, Mass and NMR spectra. With this ligand, we failed to isolate any coordination compounds with cobalt or iron metal ion but the ligand itself is non-emissive in solid or solutions even in frozen glasses at 77K.

Appendix A. Supplementary material

CCDC 762215 contains the supplementary crystallographic data for this paper. These data can be obtained free of charge from The Cambridge Crystallographic Data Center via http://www.ccdc.cam.ac.uk/data_request/cif. Supplementary data associated with this article can be found, in the online version, at doi:10.1016/j.ica.2010.03.017.

References

[1] T.J. Meyer, Acc. Chem. Res. 22 (1989) 163.
[2] (a) J. Schneider, P. Du, X. Wang, W.W. Brennessel, R. Eisenberg, Inorg. Chem. 48 (2009) 498;
(b) R. Eisenberg, D.G. Nocera, Inorg. Chem. 45 (2006) 1880;
(c) S. Chakraborty, T.J. Wadas, H. Hester, R. Schmehl, R. Eisenberg, Inorg. Chem. 44 (2005) 6865.
[3] M.D. Ward, Coord. Chem. Rev. 250 (2006) 3128.
[4] (a) C.J. Adams, N. Fey, Z. Harrison, I.V. Sazanovich, M. Towrie, J.A. Weinstein, Inorg. Chem. 47 (2008) 8242;
(b) C.J. Adams, N. Fey, J.A. Weinstein, Inorg. Chem. 45 (2006) 6105.
[5] J. Bossert, C. Daniel, Coord. Chem. Rev. 252 (2008) 2493.
[6] D.J. Stufkens, A. Vlcek, Chem. Rev. 177 (1998) 127.
[7] M. Ghosh, P. Biswas, U. Florke, K. Nag, Inorg. Chem. 47 (2008) 281.
[8] W. Kaim, A. Klein, S. Hasenzahl, H. Stoll, S. Zalis, J. Fiedler, Organometallics 17 (1998) 237.
[9] K.A. O'Donoghue, J.M. Kelly, P.E. Kruger, Dalton Trans. 13 (2004).
[10] (a) M.M. Khusniyarov, T. Weyhermüller, E. Bill, K. Wieghardt, J. Am. Chem. Soc. 131 (2009) 1208;
(b) C.C. Lu, E. Bill, T. Weyhermüller, E. Bothe, K. Wieghardt, J. Am. Chem. Soc. 130 (2008) 3181;
(c) M. Ghosh, S. Sproules, T. Weyhermuller, K. Wieghardt, Inorg. Chem. 47 (2008) 5963;
(d) N. Muresan, C.C. Lu, M. Ghosh, J.C. Peters, M. Abe, L.M. Henling, T. Weyhermüller, E. Bill, K. Wieghardt, Inorg. Chem. 47 (2008) 4579;
(e) G.H. Spikes, S. Sproules, E. Bill, T. Weyhermüller, K. Wieghardt, Inorg. Chem. 47 (2008) 10935;
(f) D. Herebian, K. Wieghardt, F. Neese, J. Am. Chem. Soc. 125 (2003) 10997;
(g) N. Muresan, T. Weyhermuller, K. Wieghardt, Dalton Trans. (2007) 4390;
(h) P. Ghosh, E. Bill, T. Weyhermüller, F. Neese, K. Wieghardt, J. Am. Chem. Soc. 125 (2003) 1293.
[11] (a) F.G.N. Cloke, C.I. Dalby, M.J. Henderson, P.B. Hitchcock, C.H.L. Kennard, R.N. Lamb, C.L. Raston, Chem. Commun. (1990) 1394;
(b) F.G.N. Cloke, G.R. Hanson, M.J. Henderson, P.B. Hitchcock, C.H.L. Kennard, C.L. Raston, Chem. Commun. (1989) 1002;
(c) M.G. Gardiner, G.R. Hanson, M.J. Henderson, v Lee, L.C. Raston, Inorg. Chem. 33 (1994) 2456.
[12] (a) A.S. Roy, N. Muresan, H.M. Tuononen, S.P. Rath, P. Ghosh, Dalton Trans. (2008) 3438;
(b) A.S. Roy, H.M. Tuononen, S.P. Rath, P. Ghosh, Inorg. Chem. 46 (2007) 5942.
[13] See, for example: (a) R.J. Baker, R.D. Farley, C. Jones, D.P. Mills, M. Kloth, D.M. Murphy, Chem. Eur. J. 11 (2005) 2972;
(b) M. Kaupp, H. Stoll, H. Preuss, W. Kaim, T. Stahl, G. Van Koten, E. Wissing, W.J.J. Smeets, A.L. Spek, J. Am. Chem. Soc. 113 (1991) 5606;
(c) T. Pott, P. Jutzi, B. Neumann, H.G. Stammler, Organometallics 20 (2001) 1965;
(d) C. Corvaja, L. Pasimeni, Chem. Phys. Lett. 39 (1976) 261;
(e) S. Richter, C. Daul, A. Zelewsky, Inorg. Chem. 15 (1976) 943.
[14] SHELXTL V.5, Siemens Analytical X-Ray Instruments, Inc., Madison, WI, USA, 1994.
[15] G.M. Sheldrick, SHELXL97, University of Göttingen, Germany, 1997.
[16] M.J. Frisch, G.W. Trucks, H.B. Schlegel, G.E. Scuseria, M.A. Robb, J.R. Cheeseman, J.A. Montgomery Jr., T. Vreven, K.N. Kudin, J.C. Burant, J.M. Millam, S.S. Iyengar, J. Tomasi, V. Barone, B. Mennucci, M. Cossi, G. Scalmani, N. Rega, G.A. Petersson, H. Nakatsuji, M. Hada, M. Ehara, K. Toyota, R. Fukuda, J. Hasegawa, M. Ishida, T. Nakajima, Y. Honda, O. Kitao, H. Nakai, M. Klene, X. Li, J.E. Knox, H.P. Hratchian, J.B. Cross, V. Bakken, C. Adamo, J. Jaramillo, R. Gomperts, R.E. Stratmann, O. Yazyev, A.J. Austin, R. Cammi, C. Pomelli, J.W. Ochterski, P.Y. Ayala, K. Morokuma, G.A. Voth, P. Salvador, J.J. Dannenberg, V.G. Zakrzewski, S. Dapprich, A.D. Daniels, M.C. Strain, O. Farkas, D.K. Malick, A.D. Rabuck, K. Raghavachari, J.B. Foresman, J.V. Ortiz, Q. Cui, A.G. Baboul, S. Clifford, J. Cioslowski, B.B. Stefanov, G. Liu, A. Liashenko, P. Piskorz, I. Komaromi, R.L. Martin, D.J. Fox, T. Keith, M.A. Al-Laham, C.Y. Peng, A. Nanayakkara, M.

Challacombe, P.M.W. Gill, B. Johnson, W. Chen, M.W. Wong, C. Gonzalez, J.A. Pople, GAUSSIAN 03, Revision E.01, Gaussian, Inc., Wallingford, CT, 2004.

[17] (a) P. Hohenberg, W. Kohn, Phys. Rev. 136 (1964) B864;
(b) W. Kohn, L.J. Sham, Phys. Rev. 140 (1965) A1133;
(c) R.G. Parr, W. Yang, Density Functional Theory of Atoms and Molecules, Oxford University Press, Oxford, UK, 1989;
D.R. Salahub, M.C. Zerner, The Challenge of d and f Electrons, ACS, Washington, DC, 1989.

[18] (a) R. Bauernschmitt, R. Ahlrichs, Chem. Phys. Lett. 256 (1996) 454;
(b) R.E. Stratmann, G.E. Scuseria, M. Frisch, J. Chem. Phys. 109 (1998) 8218;
(c) M.E. Casida, C. Jamoroski, K.C. Casida, D.R. Salahub, J. Chem. Phys. 108 (1998) 4439.

[19] (a) A.D. Becke, J. Chem. Phys. 98 (1993) 5648;
(b) C. Lee, W. Yang, R.G. Parr, Phys. Rev. B 37 (1988) 785;
(c) B. Miehlich, A. Savin, H. Stoll, H. Preuss, Chem. Phys. Lett. 157 (1989) 200.

[20] P. Pulay, J. Comput. Chem. 3 (1982) 556.

[21] H.B. Schlegel, J. McDouall, in: C. Ogretir, I.G. Csizmadia (Eds.), Computational Advances in Organic Chemistry, Kluwer Academic, The Netherlands, 1991, pp. 167–185.

[22] P.J. Hay, W.R. Wadt, J. Chem. Phys. 82 (1985) 270.

[23] W.R. Wadt, P.J. Hay, J. Chem. Phys. 82 (1985) 284.

[24] P.J. Hay, W.R. Wadt, J. Chem. Phys. 82 (1985) 299.

[25] (a) W.J. Hehre, R. Ditchfield, J.A. Pople, J. Chem. Phys. 56 (1972) 2257;
(b) P.C. Hariharan, J.A. Pople, Theor. Chim. Acta 28 (1973) 213;
(c) P.C. Hariharan, J.A. Pople, Mol. Phys. 27 (1974) 209;
(d) V.A. Rassolov, M.A. Ratner, J.A. Pople, P.C. Redfern, L.A. Curtiss, J. Comput. Chem. 22 (2001) 976;
(e) M.M. Francl, W.J. Pietro, W.J. Hehre, J.S. Binkley, D.J. DeFrees, J.A. Pople, M.S. Gordon, J. Chem. Phys. 77 (1982) 3654.

[26] (a) G.A. Petersson, A. Bennett, T.G. Tensfeldt, M.A. Al-Laham, W.A. Shirley, J. Mantzaris, J. Chem. Phys. 89 (1998) 2193;
(b) G.A. Petersson, M.A. Al-Laham, J. Chem. Phys. 94 (1991) 6081.

[27] (a) A.D. McLean, G.S. Chandler, J. Chem. Phys. 72 (1980) 5639;
(b) R. Krishnan, J.S. Binkley, R. Seeger, J.A. Pople, J. Chem. Phys. 72 (1980) 650.

[28] N.M. O'Boyle, A.L. Tenderholt, K.M. Langner, J. Comput. Chem. 29 (2008) 839.

[29] (a) M. Cossi, N. Rega, G. Scalmani, V. Barone, J. Comput. Chem. 24 (2003) 669;
(b) V. Barone, M. Cossi, J. Phys. Chem. A 102 (1998) 1995.